Supporting Information

Oladipupo et al. 10.1073/pnas.1101321108

SI Materials and Methods

Transgenic Mouse Development. K14-Cre (NCI), $VEGF^{f/f}$, and TetON-HIF-1 (1) mice were described (2–5). These mice were serially intercrossed to generate K14-Cre:$VEGF^{f/f}$:K5-rtTA:TRE-HIF-$1\alpha^{P402/564A/N803A}$ composite mice in which exon 3 of the mouse VEGF gene is recombined in K5/14 expressing basal keratinocytes during DOX-induced HIF-1–mediated angiogenesis. This combinatorial genotype was designated TetON-HIF-1:$VEGF^{\Delta}$ in the text and $VEGF^{\Delta}$ in the figures. Littermates with the unrecombined $VEGF^{f/f}$ allele, lacking the Cre transgene, were designated as TetON-HIF-1:$VEGF^{f/f}$ in the text and $VEGF^{f/f}$ in the figures. Mice were genotyped by tail DNA PCR performed with primer pairs specific for Cre, $VEGF^{f/f}$, K,5 and TRE-human-HIF-$1\alpha^{P402A/464A/N803A}$ alleles (4). Nontransgenic (NTG) and DOX day 0 (d0) TetON-HIF-1:$VEGF^{f/f}$ mice served as baseline negative and positive controls. NTG mice treated with DOX served as additional time interval controls. DOX chow was commercially obtained (200 mg/kg chow, Bio-Serv) and provided ad libitum for transgene induction. All animal care and experimental procedures were approved by the Animal Studies Committee of Washington University in St. Louis.

Tissue Preparation for Immunofluoresence. Mice were anesthetized with 2.5% Avertin and perfused with 4% paraformaldehyde via the left ventricle. One ear was removed and placed in Optimal Cutting Temperature (OCT) medium, frozen on dry ice, and stored at −80 °C as described (6) or formalin-fixed and paraffin-embedded. Cryosections (10 μm) were cut from OCT blocks, or 5-μm sections were cut from paraffin blocks for immunostaining (see below). The second ear was fixed in cold 70% ethanol overnight or prepared for whole mount immunofluorescence as described (7). Briefly, after intracardiac 4% paraformaldehyde perfusion, the ears were postfixed for 4 h in 4% paraformaldehyde, butterflied to remove cartilage, fat and muscle, rinsed in PBS, incubated for 2 h at room temperature in blocking solution (PBS plus 0.3% Triton X-100, 5% normal goat serum, and 0.2% BSA), and immunostained.

Immunostaining. Endothelial cells were stained by using Armenian hamster anti-mouse CD31 (1:2,000; MAB1398Z; Millipore) either in single or dual immunostaining. Dual immunofluorescence for Dll4, myeloid, and endothelial cell markers used the following antibodies: Dll4 (1:500; MAB 1389; R&D Systems); CD45 (1:300; 550539; BD Bioscience), CD11b (1:2,000; 550282; BD Pharmingen) clone 7/4 (1:1,000; CL8993AP; Cedarlane Laboratories) and F4/80 (1:1,000; MCA771GA; Serotec). Dual immunofluorescence for proliferating endothelial cells was performed by using Ki67 (1:1,000; ab15580; Abcam) on cryosections permeabilized with 3% Triton X-100 for 1 h at room temperature. All primary antibodies incubations were done overnight at 4 °C. Ear tissue Dll4 immunodetection was optimized by using wash buffer containing 0.01% saponin (catalog no. 47036; Sigma) and goat serum-based antibody diluent (5% goat serum, 0.3% Triton X-100, 0.02% sodium azide in 1× PBS buffer). Notch-Dll4–activated vessels were identified with Alexa Fluor 488-labeled goat anti-rat (1:400; A11006; Molecular Probes). Endothelial cells were identified with DyLight 549-labeled Goat anti-Armenian hamster IgG (1:1,000; 127–505-160; Jackson ImmunoResearch), and myeloid cells with Alexa Fluor 488-labeled goat anti-rat (1:400; A11006; Molecular probes) conjugate for 1 h at room temperature. HIF-1α and cleaved Notch1 intracellular domain (NICD Val1744)-positive cells were detected in paraformaldehyde-fixed paraffin-embedded sections after deparaffinization in xylenes, rehydration in graded ETOH, and antigen retrieval in Bull's Eye Decloaker (BULL1000 MX; BioCareMedical). After incubation with the primary antibodies: [rabbit monoclonal anti-mouse NICD1 (1:1,000; 4147; Cell Signaling)] and [rabbit anti-mouse HIF-1α (1:20,000; EP1215Y; Epitomics)], HIF-1α and NICD signals were developed by using a tyramide signal amplification kit (T20922; Invitrogen) according to manufacturer's instructions. VEFG was identified in deparaffinized and rehydrated 5-μm ETOH-fixed paraffin sections by using chicken anti-mouse VEGF (1:100; ab14078; Abcam) and Alexa Flour 488-conjugated goat anti-chicken antibody (1:400; A11039; Molecular Probes). Nuclei were counterstained by using Slow Fade Gold with 4′,6-diaminoindole (DAPI) (S36938; Invitrogen). Mast cells were detected in 4% PFA-fixed sections stained with acidified toluidine blue. For light microscopy, tissue sections stained with toluidine blue were mounted with Permount (SP15-500; Fisher Scientific) and coverslipped.

Ear whole mounts were immunostained for microvessels by using an overnight incubation at room temperature with Armenian hamster anti-CD31 (1:500; Millipore) in antibody diluent (PBS plus 0.3% Triton X-100, and 5% normal goat serum). Tissues were rinsed in three changes of 1% Triton X-100 in PBS for 5 min followed by 4-h room temperature incubation in Dylight 594-conjugated goat anti-Armenian hamster secondary antibody (1:400; Jackson ImmunoResearch). After washing, ears were mounted and coverslipped by using ProLong Gold (P-36931; Invitrogen).

Microscopy. Microscopy images were obtained on an Olympus BX61 microscope equipped with a fully automated stage by using a DP70 color Bayer mosaic digital camera, Peltier device cooled to –10 °C, (Olympus America). Fluorescence microscopy images were obtained with a Soft Imaging Solutions FVII cooled monochrome digital camera, Peltier cooled to –10 °C (Olympus America). Ear whole mount pseudostacks were collected by using Extended Focal Imaging (EFI) (MicroSuite Version 5, Olympus Soft Imaging Solutions). EFI uses contrast algorithms to create a single in-focus image from a series of images taken at different z depths for thick specimens. Objectives used were UPlanApo10×/0.40 and 20×/0.70.

For confocal microscopy, confocal z stack images were obtained by using an Olympus FV1000 confocal microscope and an UPlanApo 100×/1.35 numerical aperture oil immersion objective. A Helium-neon laser (543/618) at 15% power was used to sequentially capture images of Alexa Fluor 594-labeled targets, using Fluoview version 1.7a software (Olympus).

PAM Quantification of Microvascular Volume and Remodeling. Longitudinal OR-PAM monitoring datasets (d0–60) acquired on each mouse were three-dimensionally coregistered and segmented with a semiautomatic algorithm developed on the platform of MATLAB Image Processing Toolbox and Signal Processing Toolbox (R2010b; Mathworks). For image registration, the d0 dataset of each mouse served as its own baseline. The entire vasculature was segmented into two categories, capillaries and noncapillary trunk vessels, based on vessel diameter and 3D connectivity. Upon segmentation, the volumes of the capillaries, trunk vessels, and total vasculature were quantified by counting the associated image voxels. Starting from the principal artery-vein pair at the base of a mouse ear, the entire vasculature consists of four orders of artery-vein pairs. Vessel diameter, length, and tortuosity were quantified on a segment of

the third-order artery-vein pair. As shown in Fig. S1, the vessel diameter was measured as the shortest transverse distance across the second bifurcation point of the selected artery-vein pair segment. The vessel length between the second and third bifurcation points was measured along the vessel axis. The vessel tortuosity was computed by the ratio of the vessel length to the linear distance between the two bifurcation points. The same artery-vein pair segment was chosen for quantification throughout the 60-d monitoring. Note that all of the parameters (including vessel volume, diameter, length, and tortuosity) measured at different time points were normalized to their baselines acquired at d0.

HIF-1 Target mRNA and Protein Expression Analysis. For target gene mRNA analysis, ear tissue lysates from 3 to 4 mice per time point were prepared as described by using TRIzol extraction protocol (catalog no. 15596–018; Invitrogen) (8). Primers for RT-PCR were designed and gene expression levels normalized to histone 3.3A as described (8). The primer sequences are listed in Table S1.

Relative HIF-1 target protein levels were determined by Mouse Angiogenesis Antibody Array (catalog no. ARY015; R&D Systems) according to manufacturer's instructions. Data presented are either from one time or three independent protein arrays. Briefly, ear tissues were homogenized in cold RIPA buffer (50 mM Tris at pH 7.4, 150 mM NaCl, 1 mM EDTA, 1% Nonidet P-40, 0.1% SDS, 1% sodium deoxycholate, 1% Triton X-100) containing freshly added 2% Protease Inhibitor Mixture (P8340; Sigma) and centrifuged at 20,800 × *g* for 15 min at 4 °C. Protein lysate concentrations were quantified by using the BCA assay kit (catalog no. 23227; Pierce) and stored at −80 °C. Total protein (200 μg) was assayed, membrane protein signals developed, and select protein spots quantified by densitometry. VEGF and PlGF tissue protein levels were determined by ELISA (catalog nos. MMV00 and MP200; R&D Systems) according to manufacturer's instructions and as described (8).

Microvasculature Density and Myeloid Cell Quantification. To quantify the tissue density of microvessels or myeloid cells, the areas of CD31(+) blood vessels, CD45(+), and CD11b(+) myeloid cells were divided by the total cellular tissue area defined by DAPI(+) nuclei in 3–4 10× fields per section per mouse (n = 3–6 mice). Areas of positive fluorescence were quantified by using image analysis software (MicroSuite Version 5).

Induction of Ear Skin Inflammation. For inflammatory challenge experiments, 2.5 μg of 12-*O*-tetradecanoylphorbol-13-acetate (TPA) (Sigma-Aldrich) were dissolved in dimethyl sulfoxide (DMSO) and topically applied to each side of the ear of $VEGF^{\Delta}$ and $VEGF^{f/f}$ mice pretreated with DOX for 14 d. Ears were harvested for immunofluorescence and protein analysis 10 d later based on previous work in our laboratory (8).

Statistical Analysis. The data are reported as the mean ± SD. Data from DOX-treated TetON-HIF-1:$VEGF^{\Delta}$ or TetON-HIF-1$VEGF^{f/f}$ mice were compared either with d0 or NTG mice treated with DOX for the same interval by using the unpaired Student t test (GraphPad Prism 5). There were 3–6 mice per group unless otherwise indicated.

1. Oladipupo SS, et al. (2011) Conditional HIF-1 induction produces multistage neovascularization with stage-specific sensitivity to VEGFR inhibitors and myeloid cell independence. *Blood* 117:4142–4153.
2. Diamond I, Owolabi T, Marco M, Lam C, Glick A (2000) Conditional gene expression in the epidermis of transgenic mice using the tetracycline-regulated transactivators tTA and rTA linked to the keratin 5 promoter. *J Invest Dermatol* 115:788–794.
3. Gerber HP, et al. (1999) VEGF is required for growth and survival in neonatal mice. *Development* 126:1149–1159.
4. Bekeredjian R, et al. (2010) Conditional HIF-1alpha expression produces a reversible cardiomyopathy. *PLoS ONE* 5:e11693.
5. Jonkers J, et al. (2001) Synergistic tumor suppressor activity of BRCA2 and p53 in a conditional mouse model for breast cancer. *Nat Genet* 29:418–425.
6. Lu K, Lamagna C, Bergers G (2008) Chapter 3. Bone marrow-derived vascular progenitors and proangiogenic monocytes in tumors. *Methods Enzymol* 445:53–82.
7. Elson DA, et al. (2001) Induction of hypervascularity without leakage or inflammation in transgenic mice overexpressing hypoxia-inducible factor-1alpha. *Genes Dev* 15: 2520–2532.
8. Scortegagna M, et al. (2008) HIF-1alpha regulates epithelial inflammation by cell autonomous NFkappaB activation and paracrine stromal remodeling. *Blood* 111: 3343–3354.

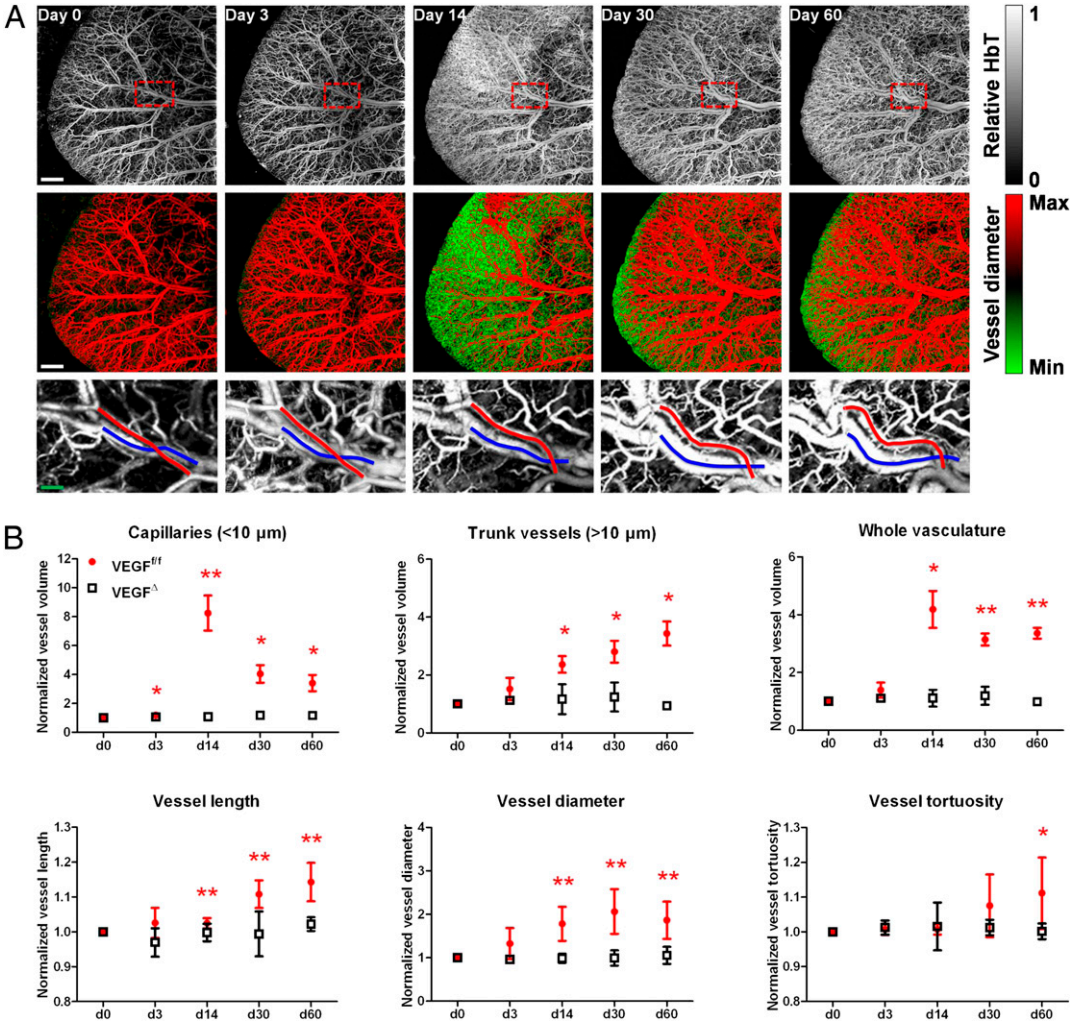

Fig. S1. Optical-resolution photoacoustic microscopy and 3D vessel segmentation analysis. (*A*) (*Top*) Representative OR-PAM maximum-amplitude-projection images of the entire ear vasculature of a longitudinally imaged VEGF$^{f/f}$ mouse treated with DOX for 60 d. (Scale bar: 1 mm.) (*Middle*) Differentiation between capillaries and trunk vessels via vessel segmentation. Capillaries are false-colored green and trunk vessels red. (Scale bar: 1 mm.) (*Bottom*) Quantification of trunk vessel remodeling (i.e., length, vasodilatation, and tortuosity) in a pair of selected arterial-venous segments. Red and blue solid curves indicate the vessel axes of the arterial and venous segments, respectively. (*B*) Quantification of *A* showing microvascular multiparameter measurements from days 0 to 60 ($n = 3$ mice per time point, see *Materials and Methods* for more details). VEGF$^{f/f}$ or VEGF$^{\Delta}$ data at each DOX day were compared with VEGF$^{f/f}$ day 0 data by using the unpaired Student t test (*$P < 0.05$, **$P < 0.01$, and ***$P < 0.001$). (Scale bar: 200 μm.)

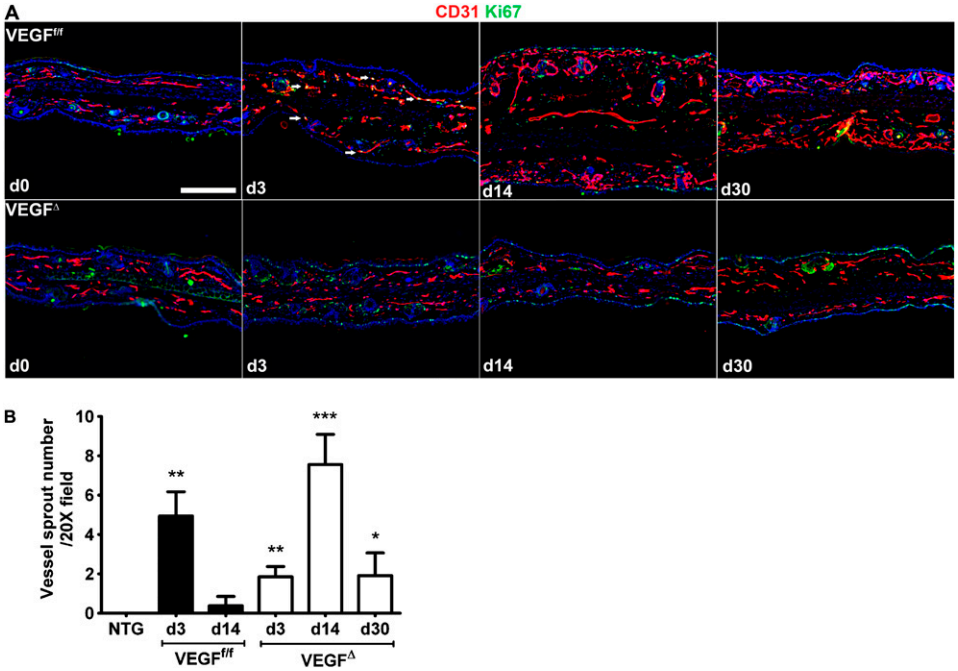

Fig. S2. VEGF is required for HIF-1–mediated endothelial proliferation. (*A*) Representative dual CD31/Ki67 immunofluorescence reveals lack of double-positive endothelial cells in VEGF$^{\Delta}$ mice from d0–30. In contrast, double-positive VEGF$^{f/f}$ endothelial cells markedly increased by d3 and decreased to near baseline levels by d14. (*B*) Quantification of endothelial sprouting as presented in Fig. 3*A*, *Left*. Data analyzed as in Fig. 1: *$P < 0.05$, **$P < 0.01$, and ***$P < 0.001$. (Scale bar: 200 μm.)

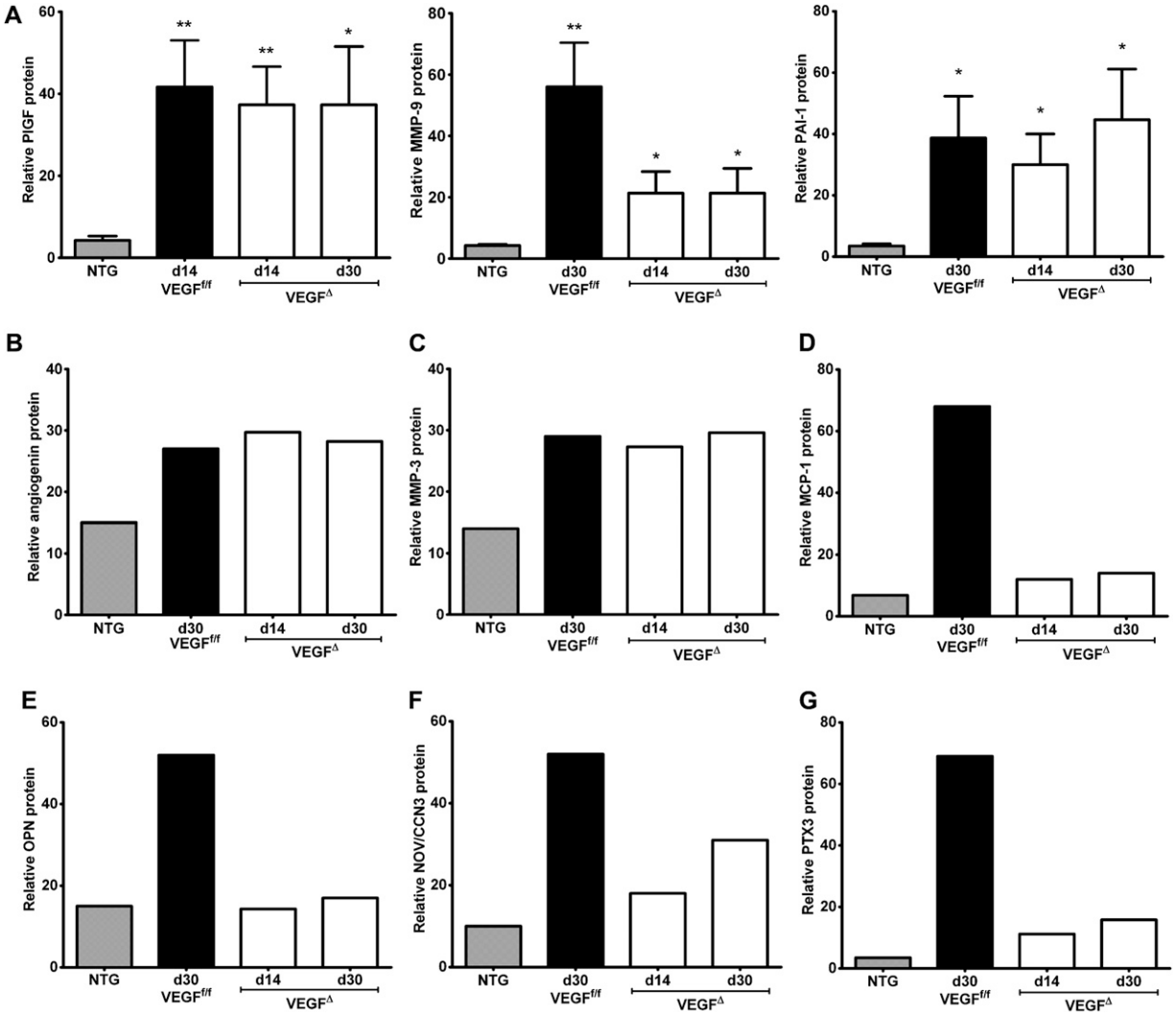

Fig. S3. Angiogenesis antibody array analysis of HIF-1 angiogenic and immune cell mediators. Angiogenesis antibody arrays were performed in duplicate in either a single (*D*–*G*) or three independent experiments (*B*–*G*) with tissue extracts from nontransgenic (NTG), VEGF$^{\Delta}$, or VEGF$^{f/f}$ mice. (*A*–*C*) PlGF, MMP-9, PAI-1, angiogenin, and MMP-3 were up-regulated in VEGF$^{\Delta}$ mice to similar levels as VEGF$^{f/f}$ controls. (*D*–*G*) Osteopontin (OPN), pentraxin-3 (PTX-3), cysteine rich 61/connective tissue growth factor/nephroblastoma overexpressed gene (CCN3/NOV), and macrophage chemoattractant protein-1 (MCP-1) induction was markedly impaired despite striking up-regulation of other HIF-1 targets in VEGF$^{\Delta}$ mice. Data analyzed as in Fig. 1: $*P < 0.05$, $**P < 0.01$, and $***P < 0.001$.

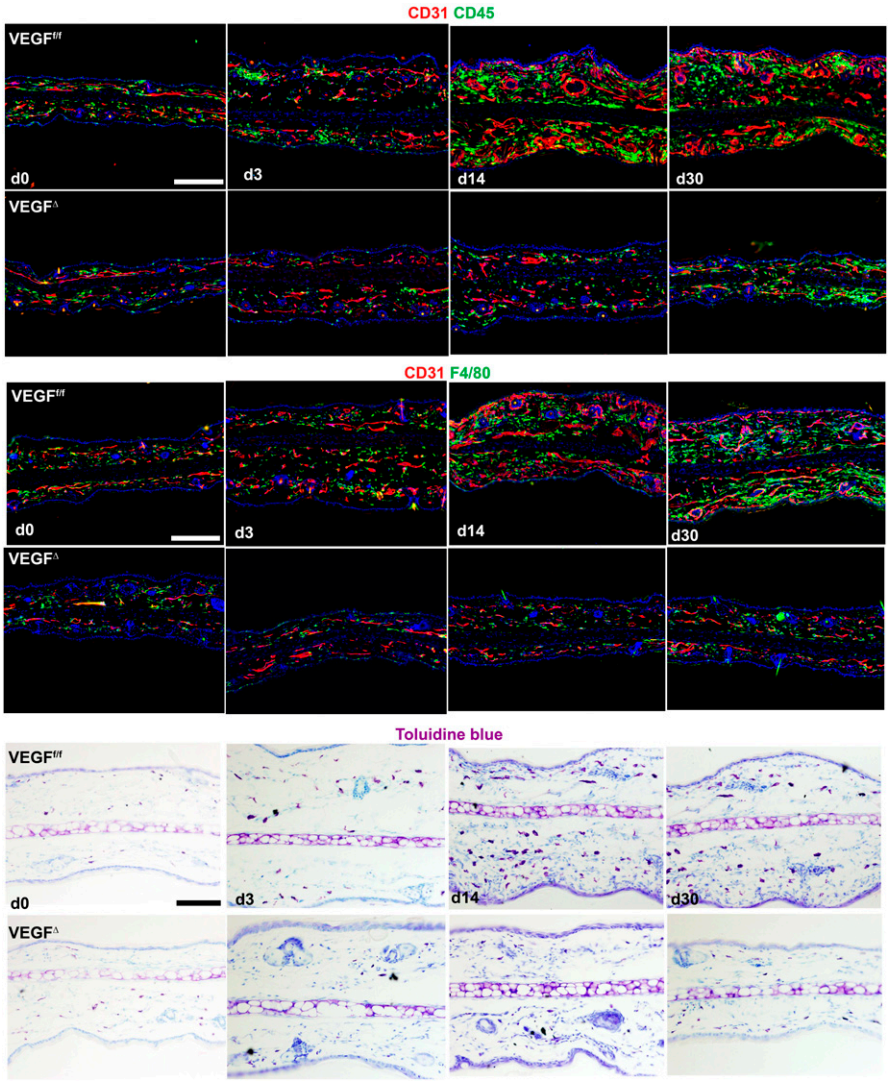

Fig. S4. Loss of epithelial VEGF impairs macrophage and mast cell infiltration. Representative CD31/CD45 or F4/80 dual immunofluorescence and toluidine staining demonstrating lack of CD45, F4/80 myeloid, and mast cell recruitment in d14 VEGF$^{\Delta}$ mice. By d30, VEGF$^{\Delta}$ mice evidenced a small increase in CD45 myeloid and mast cells. (Scale bars: CD45 and F4/80, 200 μm; Toluidine staining, 100 μm.)

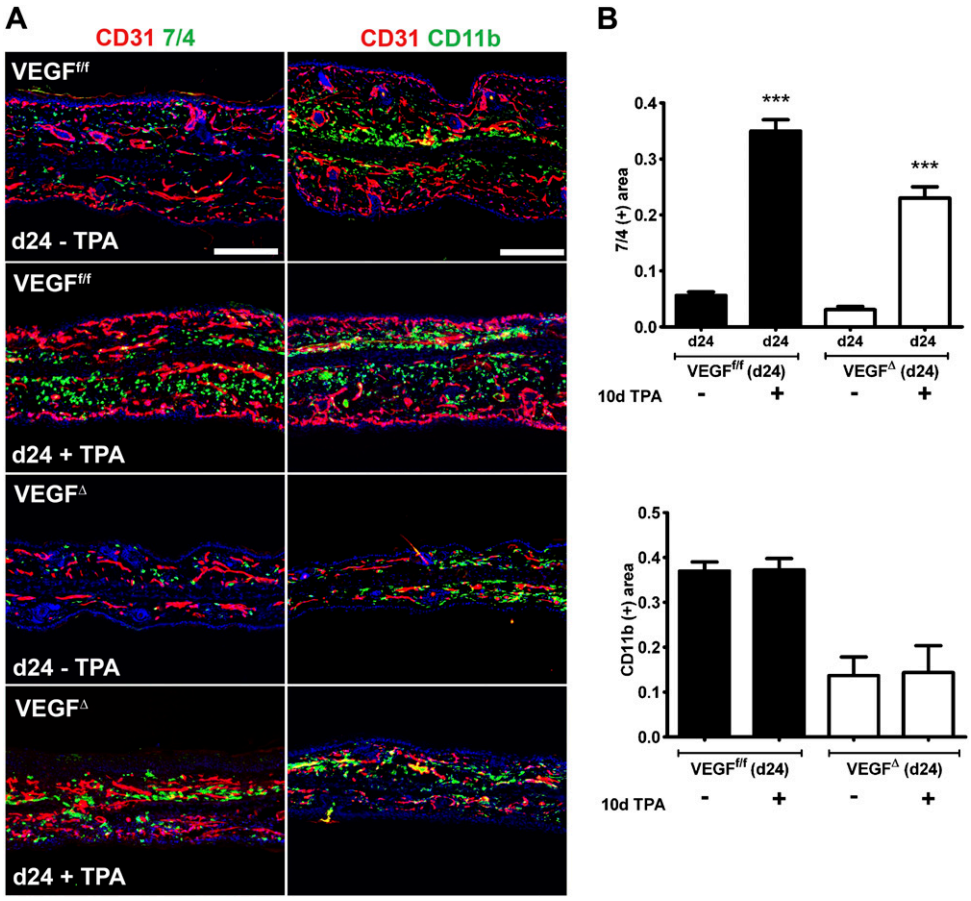

Fig. S5. TPA induction produces partial rescue of neovascularization. (*A*) A single topical TPA dose in VEGF$^{\Delta}$ mice produced a marked influx of 7/4 (+) stromal neutrophils to levels similar to DOX-treated VEGFf/f mice, and a partial rescue of neovascularization. TPA did not affect the enhanced neovascularization of VEGF$^{f/f}$ mice or stromal neutrophil infiltration. CD11b recruitment was unaffected by TPA treatment either in VEGF$^{\Delta}$ or VEGF$^{f/f}$ mice. (*B*) Quantification of *A, Left* [7/4(+) area] and *Right* [CD11b(+) area]. (n = 3–6 mice per time point). Data analyzed as in Fig. 1: $^{*}P < 0.05$, $^{**}P < 0.01$, and $^{***}P < 0.001$. (Scale bars: 200 μm.)

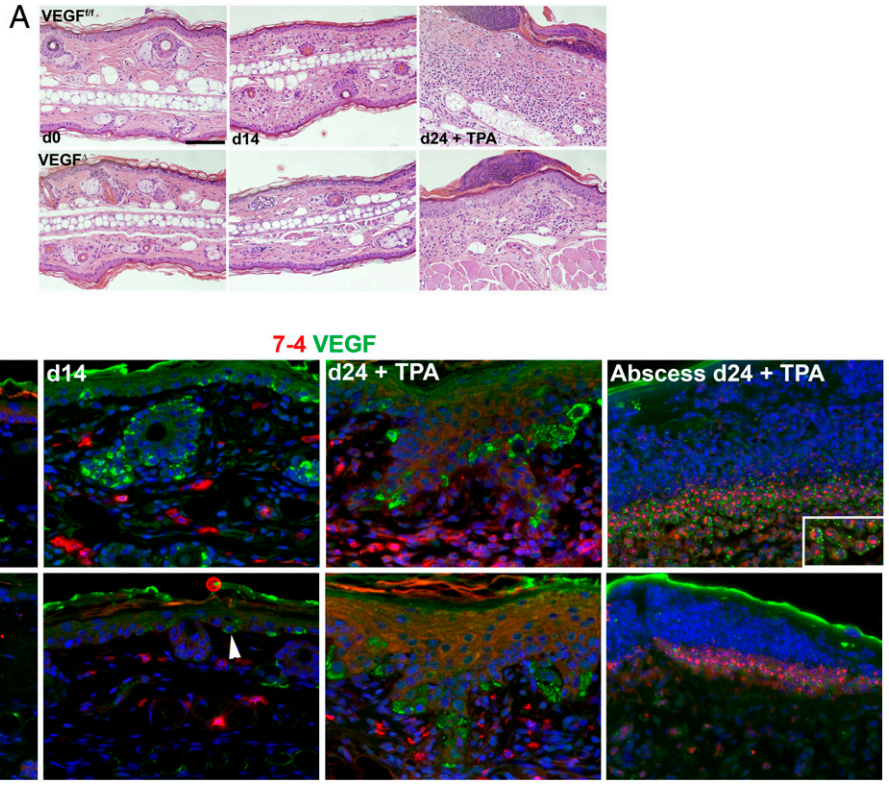

Fig. S6. Topical TPA enhances and prolongs inflammatory response in VEGF$^{f/f}$ and VEGF$^{\Delta}$ mice. (*A*) Epidermal neutrophil abscesses 10 d after TPA challenge in both DOX d14 VEGF$^{f/f}$ and VEGF$^{\Delta}$ mice (*Right*). Accumulation of inflammatory cells is also evident throughout the stroma in both VEGF$^{f/f}$ and VEGF$^{\Delta}$ TetON-HIF-1 mice. TetON-HIF-1:VEGF$^{\Delta}$ mice do not recruit inflammatory cells after 14 d of HIF-1 induction in contrast to DOX d14 TetON-HIF-1:VEGF$^{f/f}$ counterparts. (*B*) Representative dual 7/4-VEGF immunofluorescence, showing stromal 7/4(+) neutrophils in both VEGF$^{f/f}$ and VEGF$^{\Delta}$ mice (first three columns). Surprisingly, the source of ear VEGF in TPA-treated VEGF$^{\Delta}$ mice was from the epidermis (third column) and abscess-derived 7/4(+) neutrophils (fourth column and *Inset*), rather than the stromal 7/4(+) cells (third column) (Scale bars: *A*, 100 μm; *B*, 50 μm.)

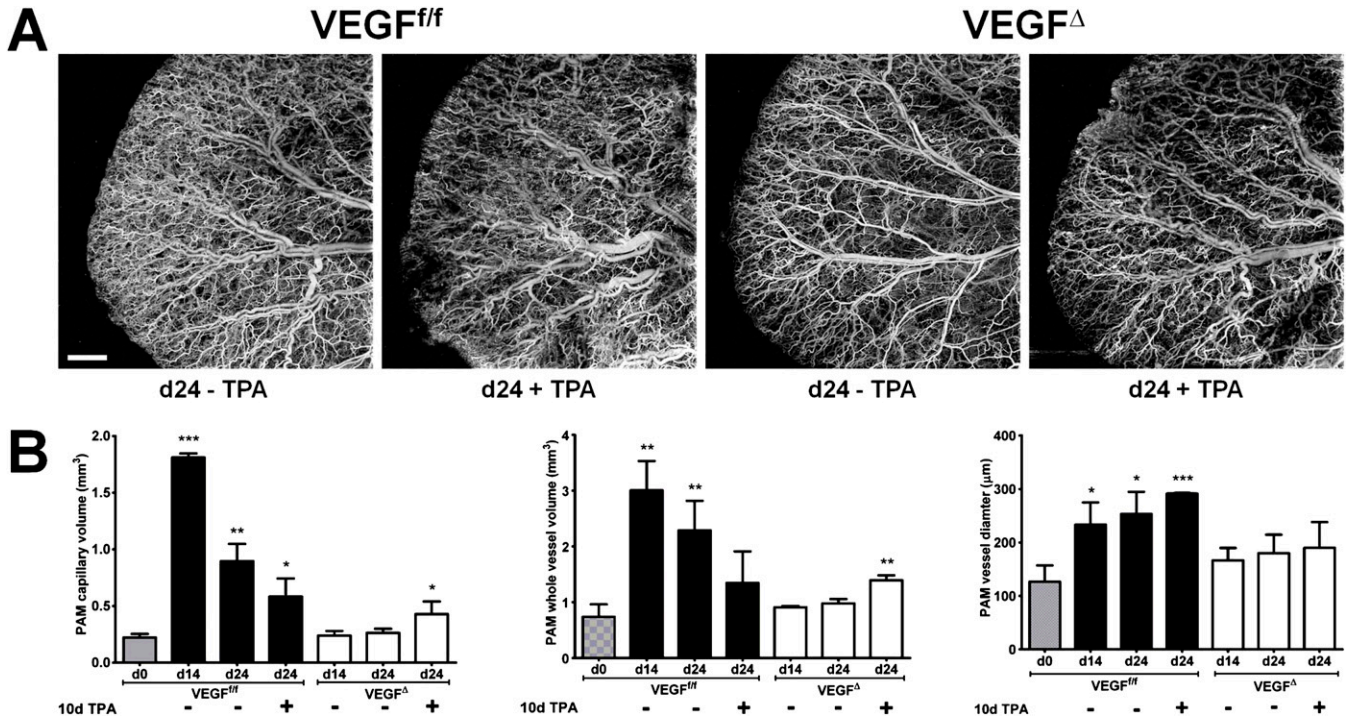

Fig. S7. Topical TPA rescues HIF-1 neovascularization in VEGF$^{\Delta}$ mice. (*A*) Angiogenesis determination and accompanying vascular remodeling in TPA-treated and nontreated VEGF$^{f/f}$ and VEGF$^{\Delta}$ mice by OR-PAM. TPA partially rescued both capillary volume and arteriovenous remodeling. (*B*) Quantification of vascular parameters in *A* ($n = 3$ mice, see *Materials and Methods* for more details). Data analyzed as in Fig. 1: $^{*}P < 0.05$, $^{**}P < 0.01$, and $^{***}P < 0.001$. (Scale bar: 500 μm.)

Table S1. Real-time primer-probe sets used for RT-PCR analysis of HIF-1 target gene expression

Primers	Sequences
Mouse Dll4	
Forward	GACCTGCGGCCAGAGACTT
Reverse	GCCAAATCTTACCCACAGCAA
Primer probe	CCAGGAAACTCTCTCATCAGCCAAATCATCA
Mouse Hey1	
Forward	GGCAGCAAGCAAGACAGTTATGT
Reverse	CGGTGAAATCCGTGAGACTGA
Primer probe	CCTGCACTTGGCAGCCCTAAGCACT
Mouse VEGF	
Forward	GCAGGCTGCTGTAACGATGA
Reverse	GTGAGGTTTGATCCGCATGA
Primer probe	CCCTGGAGTGCGTGCCCA
Mouse ADM	
Forward	AAGCCCACATTCGTGTCAAAC
Reverse	GAAGCGGCATCCATTGCT
Primer probe	CTACCGCCAGAGCATGAACCAGGG
Mouse iNOS	
Forward	TGACGGCAAACATGACTTCAG
Reverse	GCCATCGGGCATCTGGTA
Primer probe	TTCACAGCTCATCCGGTACGCTGG
Mouse CAIX	
Forward	GATTCTCGGCTACAACTGA
Reverse	GGGAAGGAAGCCTCAATCGT
Primer probe	TCCGAGCCACGCAACCCTTGA
Mouse histone 3.3A	
Forward	CGTGAAATCAGACGCTATCAGAA
Reverse	TCGCACCAGACGCTGAAAG
Primer probe	TCCACTGAACTTCTGATCCGCAA